



Original article

## Computational structural integrity analyses of a canard box-wing unmanned aerial vehicle (UAV) platform for disaster management and agricultural surveillance applications

Patadlas, Aiza A.<sup>1\*</sup>, Remocaldo, Genesis N.<sup>2</sup>, Ambos, Edgar C.<sup>3</sup>, Galindo, Ronald M.<sup>3</sup>, Maglasang, Jonathan C.<sup>1</sup>

<sup>1</sup>Mindanao State University – Iligan Institute of Technology, 9200 Iligan City

<sup>2</sup>Air Force Research and Development Center, Philippine Air Force, Clark, 2009 Pampanga

<sup>3</sup>Cebu Technological University - Main Campus, 6000 Cebu City

### ABSTRACT

The modern concern on energy, efficiency and environment leads to the development of unconventional designs of an unmanned aerial vehicle (UAV) platform of box-wing configuration for agricultural surveillance, risk and disaster management and other civilian applications. The box-wing configuration used in this study was based on Prandtl's best wing system which gives the smallest possible induced drag for a given wing span and height. In this study, the structural integrity of the designed UAV was evaluated using finite element method software. The aerodynamic loads resulting from the computational fluid dynamics (CFD) simulations were exported to the finite element method solver in SolidWorks™ for stress analyses. The maximum stresses with and without gust are  $1.726 \times 10^7 N/m^2$  and  $7.36 \times 10^6 N/m^2$ , respectively, which are still below the rupture strength of Balsa wood which is at  $2.1 \times 10^7 N/m^2$ . The designed UAV was equipped with a spring-damper system in order to avoid severe damage due to impact forces during landing. The front and aft wings have flutter speeds of  $37.23 m/s$  and  $30.164 m/s$ , respectively. The designed Prandtl box-wing was able to reach  $2.438 \times 10^6$  cycles. When a wind gust of  $5 m/s$  was introduced in a cyclic fashion the load factor  $n$  reaches 2.5 but still without detrimental effects being observed in the structure. The overall computational fluid dynamics and structural analyses results showed that the designed box-wing UAV for efficient disaster management and surveillance applications could perform well and withstand the projected loading conditions during various flight missions.

**KEYWORDS:** *computational fluid dynamics, finite element method*

### 1 INTRODUCTION

An Unmanned Aerial Vehicle (UAV) takes its pride as it is called “an eye in the sky”, is a pilotless aircraft designed to conduct surveillance to provide assessment and overview of a time sensitive situation with high accuracy and precision. Its applications have grown so much from providing advancement in military exercises to increasing the productivity of a civilian oriented task especially in agriculture. Depending on the desired application and mission profile, UAVs are usually built with integration of cameras and sensors for monitoring and data gathering. For example, the designed UAV being used in this study is capable of carrying various payloads and to answer the need for an aerial system to perform real-time data acquisition in a risk and disaster management operation [6 and 7] as well as in agricultural applications such as crop monitoring and pesticide spraying [20,25, and 29].

The applications of UAVs in the agricultural sector in the Philippines may include monitoring of crop production, soil health evaluation, providing assistance in the irrigation process, applying fertilizers and pesticides, etc. The use of UAVs reduces the risk that the farmer is likely to experience. “The adoption of modern technologies in agriculture, such as the use of drones or unmanned aerial vehicles (UAVs) can significantly enhance risk and damage assessments and revolutionize the way we prepare for and respond to disasters that affect the livelihoods of vulnerable farmers and fishers and the country’s food security.” said José Luis Fernández, FAO Representative in the Philippines.

UAVs have been known as well for a long time now as a “humanitarian in the sky” assisting Local Government Units (LGUs) to locate the areas that are badly hit by the calamity to provide immediate assistance and assessment of the situation. They have been very helpful in providing the necessary data in the distribution of goods, medicines and materials, when roads are unpassable and when communication is down, they can be easily deployed to exchange information [14].

Compared to the existing drones that the agricultural field is using today, the designed UAV in this study is a

\*corresponding author: [aiza.albufera88@gmail.com](mailto:aiza.albufera88@gmail.com)

p-ISSN: 2599-4875 e-ISSN: 2599-4980

©Cebu Technological University, R. Palma St. corner M.J. Cuenco Ave., Cebu City, 6000 Philippines

fixed-wing UAV utilizing the best wing system theory of Ludwig Prandtl that a box-wing configuration aircraft accumulates a much smaller induced drag compared to a monoplane [9]. The entire configuration will be made of Balsa wood as well which is currently not done yet. This UAV also falls under the category of a close-range mini UAV which cruises at a sub-sonic range of Mach number  $M = 0.05$ . It is incorporated with canard wings which act as horizontal stabilizers integrated at the front of the fuselage to improve the stability and minimize the complexity of the controls of the box-wing configuration while further improving the aircraft's agility and maneuverability.

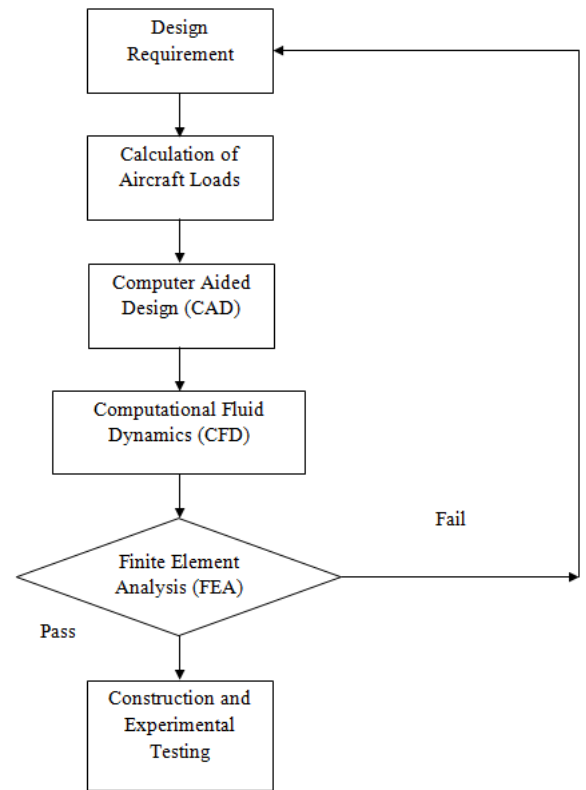
The aerodynamics analysis conducted on the designed UAV in the previous studies showed that it is 25% more efficient compared to the referenced conventional aircraft [18]. That substantial efficiency difference in favor of the canard box-wing configuration over the conventional UAV design is the main reason why such configuration has great potential for adoption in long range and long duration applications such as in disaster management and agricultural surveillance.

In this study, the designed canard box-wing unmanned aircraft was evaluated for its structural integrity. That is, if it could withstand the various imposed loading conditions in the mission profile of the aircraft while still satisfying the desired design parameters. It is in this study that the flight envelope that covers the application limits of the aircraft was generated. It provides the safety margin needed to control the aircraft from its take-off flight to landing.

**2 MATERIALS AND METHODS**

**2.1 Design Requirements**

The design requirements of an aircraft are generally specified by the customer based on the aircraft's intended application and desired mission profile. The specifications are gathered directly from the customers themselves, that is, depending on how the customer will select its aircraft's system. The selection includes and is not limited to the vehicle's payload, endurance, radius of action, speed range, how it is launched and recover, etc. These customers vary widely from civilian to military individuals and its application is either for recreational or reconnaissance. For this study, table I provides the generalized design requirements of a close-range mini UAV along with its desired mission profile in Figure 2 [19].



**I Design requirement for a close-range mini UAV.**

Gross Weight	4 - 7 kg
Wing Span	1.5 - 2.5 m
Cruise Speed	20 - 25 m/s
Endurance	1 hour
Operating Range	10 km
Payload Mass	1 - 1.5 kg

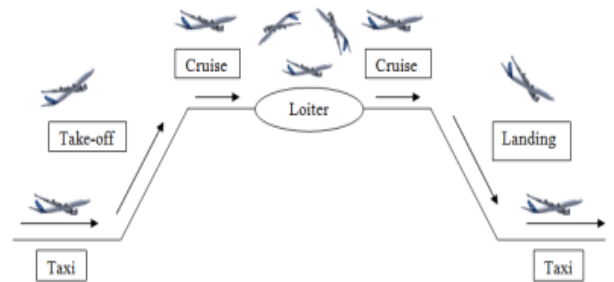


**Figure 2 Desired mission profile.**

**2.2 Calculation of Aircraft Loads**

The aircraft is expected to be able to withstand any time loads are applied on it during the course of its operation. Even when it is on the ground it is subjected by its own weight, which is acting at the undercarriage. This load is then transmitted on the principal structures of the aircraft. In this study, calculations of aircraft loads

during maneuvers such as level flight, steady pull-up and pull down and correctly banked turn were conducted and the results were used as bases for constructing the V-n diagram which provides the operation limit of the UAV.

For a steady, level flight,  $Lift (L) = Weight (W)$  and  $Thrust (T_R) = Drag(D)$ . Lift is an aerodynamic force developed due to the pressure difference between the upper and lower surfaces of an aircraft. Thrust is a force provided by its power plant which counters the drag that the aircraft is experiencing, a force generated when air is disrupted along its motion. These forces are illustrated and evaluated as follows:

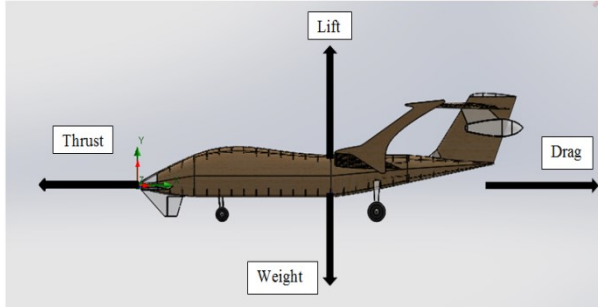


Figure 3 Steady level-flight aerodynamic forces of the designed UAV

$$L = C_L qS \quad (1)$$

$$D = C_D qS \quad (2)$$

$$T_R = \frac{W}{L/D} \quad (3)$$

It was assumed that the aircraft will experience a sharp and graded gust. This is an atmospheric disturbance that is highly unavoidable during flight. The lowest speed at which the maximum load factor can be reached corresponds to the point of intersection of the positive stall curve and the limit load. The maximum allowable speed denoted as  $V_D$  is  $\geq 1.25 V_C$ ; ( $V_C$  is the cruise speed of the vehicle).  $V_A$  is the corner speed which was determined using the equation:

$$V_A = \sqrt{\frac{2n_{max} W}{\rho C_{Lmax} S}} \left(\frac{m}{s}\right) \quad (4)$$

where  $n_{max}$  is the maximum load factor,  $W$  is the weight of the aircraft, and  $C_{Lmax}$  is the maximum coefficient of lift. Additionally, for equations 1 to 3,  $q$  is the dynamic pressure,  $\rho$  is the air density,  $V$  is the true air speed,  $C_L$  is the coefficient of lift,  $C_D$  is the coefficient of drag, and  $S$  is the wing surface area.

Another critical aspect that was evaluated is the performance of the aircraft during landing. A spring-damper system was incorporated in the design to avoid failure and critical damage on the aircraft especially during hard landing. This process allows the designers to determine the necessary number and correct dimensions and spacing of the spars, ribs and skin [5, 11, and 13].

Figure 35 shows the diagram of a spring damper system.

$$m\ddot{x}(t) + c\dot{x}(t) + kx(t) = 0 \quad (5)$$

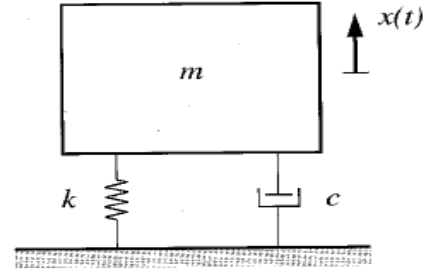


Figure 4 Spring damper system (Meirovitch, 2001).

Flutter is considered as the vibration of the structure. In this study, flutter analysis was conducted only on the wings. Flutter is generated when aerodynamic forces interact with structural stiffness. The equation of motion for the wing that experience fluid flow is given by the following equations:

$$\left\{ \frac{m}{\pi \rho_{\infty} b^2} \left[ 1 - \left( \frac{\omega h}{\omega} \right)^2 \right] + I_h(k, M_{\infty}) \right\} \ddot{\theta} + \left[ \frac{m x_{\theta}}{\pi \rho_{\infty} b^2} + I_{\theta}(k, M_{\infty}) \right] \dot{\theta} = 0 \quad (6)$$

$$\left\{ \frac{m x_{\theta}}{\pi \rho_{\infty} b^2} + m_h(k, M_{\infty}) \right\} \ddot{\theta} + \left\{ \frac{I_p}{\pi \rho_{\infty} b^4} \left[ 1 - \left( \frac{\omega \theta}{\omega} \right)^2 \right] + m_{\theta}(k, M_{\infty}) \right\} \dot{\theta} = 0 \quad (7)$$

The repeated loading and unloading weakens the object/s over time even if the induced stresses are considerably less than the allowable stress limits. This phenomenon is known as fatigue. Each cycle of stress fluctuation weakens the object to some extent. After a number of cycles, the object becomes so weak that it fails. The failure prediction method used was Von Mises stress. It determines if the material will yield or will suffer fracture. It was chosen because it was available in SolidWorks simulation. The method used in conducting fatigue analysis in this study is the Soderberg method – generally the most conservative and is given by the equation:

$$S_{ca} = \frac{S_y S_a}{S_y - S_{mean}} = \frac{S_a}{1 - \left( \frac{S_{mean}}{S_y} \right)} \quad (8)$$

where  $S_a$  is the alternating stress and  $S_y$  is the yield stress.

### 2.3 Computer Aided Design (CAD)

Computer Aided Design (CAD) is a computer program widely used by design engineers and researchers nowadays to improve the design phase allowing them to create even complex designs and avoid unnecessary rework. In this study, a CAD-embedded program called SolidWorks™ was used to model and render three-dimensional designs of the UAV structures. When the aircraft loads were determined, the 3D models of the aircraft's structures were sketched in CAD and used in the computational fluid dynamics (CFD) and structural analyses. The models were immediately improved whenever there was failure in any of the structural integrity requirements of the components.

## 2.4 Computational Fluid Dynamics (CFD)

Computational fluid dynamics (CFD) analysis is used to evaluate the different fluid forces and their effects on the design by performing a computer fluid flow simulation. In this study, the model was loaded to the flow simulation environment of SolidWorks™. The type of flow analysis selected was external and with air as the fluid. The boundary limits were specified at the inlet and outlet of the flow. The mesh setting was at medium and the drag and lift forces were modeled to act along the x and y coordinates, respectively. It is important to note that in order to acquire reliable results, correct boundary conditions like flow velocity and appropriate meshing level must be set before running the analysis.

## 2.5 Finite Element Analysis (FEA)

The structural integrity of the UAV for the various loading conditions was evaluated using SolidWorks™ finite element method (FEM) solver after importing the results from the CFD analysis. This method of finite element analysis is usually done to avoid excessive cost due to frequent changes in the design.

The material properties of balsa wood provided by SolidWorks™ were used in analyzing the configuration. Boundary conditions were chosen carefully so that the analysis would be consistent and closer to the real case scenario. In stress analysis, the whole configuration was subjected to static loading with and without the introduction of gust. However, due to the complexity of the canard and box-wing configuration design and the limitation of the performance of the used computer, only the wings were analyzed for dynamic loading. Nodal deflections due to twisting and bending of the front and aft wings due to the dynamic loading were analyzed. Since the SolidWorks™ vibration analysis solver is only capable of determining the natural frequencies; flutter speed was determined by manual calculations. For the fatigue analysis, the wings were simulated using the limit load and gust load to determine the life cycle. Lastly, for the impact test, motion analysis was used to evaluate the landing performance of the aircraft. Forces and the corresponding stresses were then determined. During the design and analyses iterations, when one of the components failed, the UAV model and design requirements were re-evaluated and adjusted to start again the iterative processes until the UAV met the design requirements as aerodynamically and structurally sound aerial vehicle.

## 2.6 Material Used

The material used in the analysis is balsa wood. It has good characteristics in terms of strength to weight

ratio and it can also easily be formed and crafted with rapture strength of 21.6 MPa [27]. The mechanical properties of balsa wood generated from SolidWorks™ for linear elastic isotropic model are shown in Table II. Figure 3 then is an example of Balsa wood that can be bought in the market today.

II Mechanical properties of Balsa Wood.

Balsa Wood	
Density	$160 \pm 10 \text{ kg/m}^3$
Elastic Modulus	$3 \times 10^9 \text{ Pa}$
Shear Modulus	$3 \times 10^8 \text{ Pa}$
Yield Strength	20 MPa
Thermal Conductivity	0.05 W/(m.K)



Figure 5 Balsa wood [shorturl.at/clsS3].

## 3 RESULTS AND DISCUSSIONS

Figure 4 shows the V-n diagram (flight envelope) of the designed UAV. The limiting values are 1.4 and -1.09 which correspond to the positive and negative load factors, respectively. The  $V_{stall} = 14.5 \text{ m/s}$  which was specified from the aerodynamic analysis, is the speed at which the load factor  $n = 1$ . The  $V_A = 17.2345 \text{ m/s}$  in the upper left corner of the diagram is the maximum speed at which the aircraft can be flown at maximum coefficient of lift  $(C_L)_{max}$ . Speeds higher than  $V_A$  could potentially result to structural failures. To be able to increase the velocity up to  $V_B = 20 \text{ m/s}$  which is the designed cruise speed, the coefficient of lift must be less than the maximum. This means that the vehicle should not be forced to undergo rapid steep climb during its operation. Line AB denotes the positive load factor. At the right side of the V-n diagram, the cut-off lines  $BD_1$  and  $D_2E$  provides the boundary of the design since it is not ideal to apply the limit loads at maximum speed  $V_D = 25 \text{ m/s}$ . The negative load factor was determined from the maximum negative coefficient of lift from the aerodynamic analysis. When a gust of  $5 \text{ m/s}$  was introduced, the load factor reached 2.5. Based on the FEA analysis conducted, there were no detrimental effects observed in the structure. However, it is not recommended to go beyond the flight envelope since it is possible that destructive phenomena such as flutter may occur which could result to sudden structural failure

of the UAV.

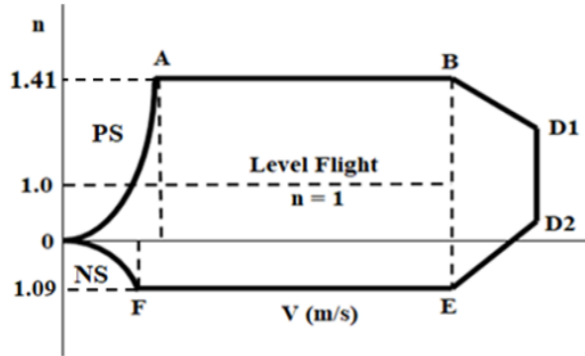


Figure 6 V-n diagram of the designed UAV.

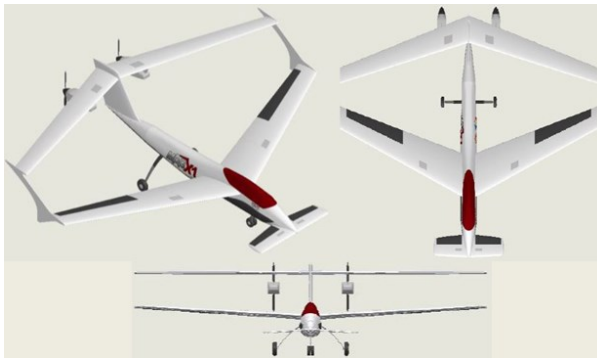


Figure 7 3D sketch of the designed canard box-wing MAG X1 [19].

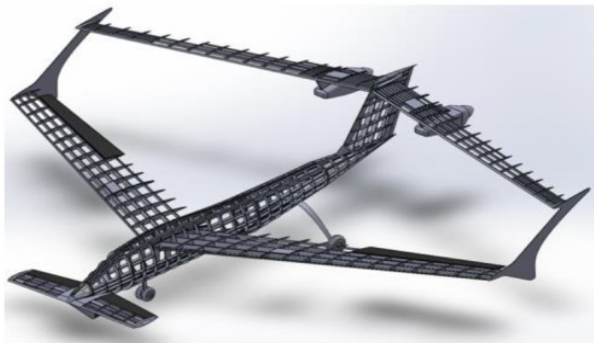


Figure 8 MAG X1 platform structural layout plan [19].

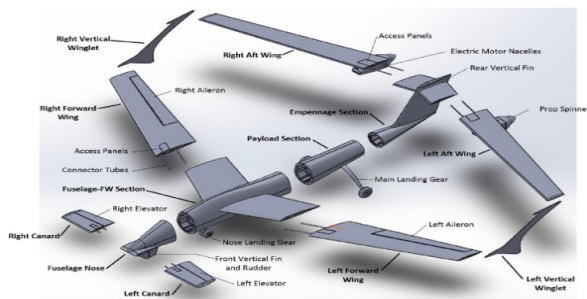


Figure 9 Exploded view of the MAG X1 major parts for disassembly [19].

The final design of the canard-configured Prandtl

plane UAV which was named MAG X1 is shown in Fig. 7. Its structural layout was carefully designed and is illustrated in Figures 8. And for ease of transportation, the UAV was designed with features that its major parts and components are easily disassembled as shown in Figure 9, but without compromising its structural integrity.

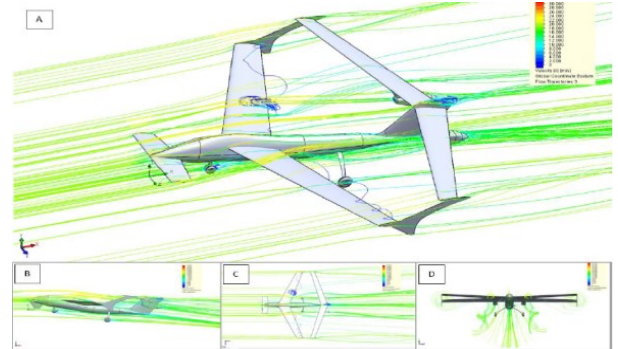


Figure 10 CFD analysis fluid flow visualization [19].

After thorough calculation and sketching, CFD analysis was conducted to the UAV model. The CFD analysis determined the effects of the aerodynamic loadings and the performance of the configuration designs as shown in Figure 10.

The results from the CFD simulations were then loaded into a finite element solver in SolidWorks™ to determine the responses of the structure from the applied forces. Figure 11 shows that stress concentrations occur primarily at the connection of the wings and the fuselage, as expected. The maximum stresses with gust of 5 m/s and without gust are  $1.726 \times 10^7 \text{ N/m}^2$  and  $7.436 \times 10^6 \text{ N/m}^2$ , respectively. These are the stresses that the model experienced during simulations. The basis for the conclusion of the model's efficiency was based on these stresses. The maximum stress occurs at node 7063 of the wing-fuselage connector. The maximum deflections of the aft and front wings for both static and dynamic loadings are tabulated then in Table III.

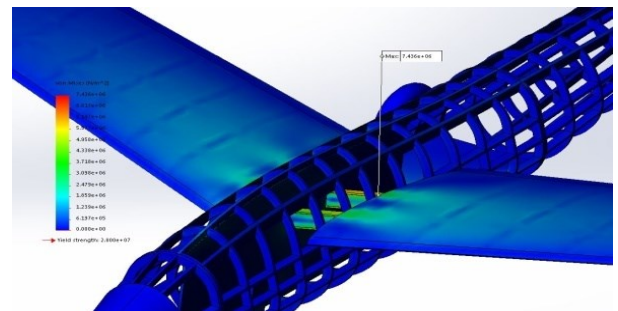


Figure 11 Wing stresses from FEA on the UAV (SolidWorks).

III Maximum deflections experienced by the UAV

wings.

Maximum Deflection							
Static Loading				Dynamic Loading			
Node	Bending	Node	Twisting	Node	Bending	Node	Twisting
17926	18.365 mm	475390	18.525 mm	11428	18.183 mm	115672	18.741 mm
81574	17.543 mm	275914	17.922 mm	23921	17.563 mm	30599	18.097 mm

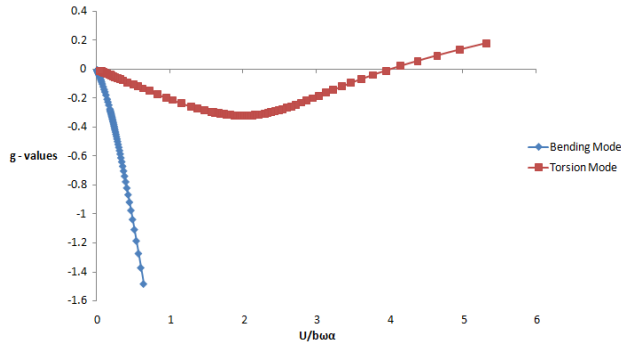


Figure 12 U-g and U-frequency diagram for the front wing.

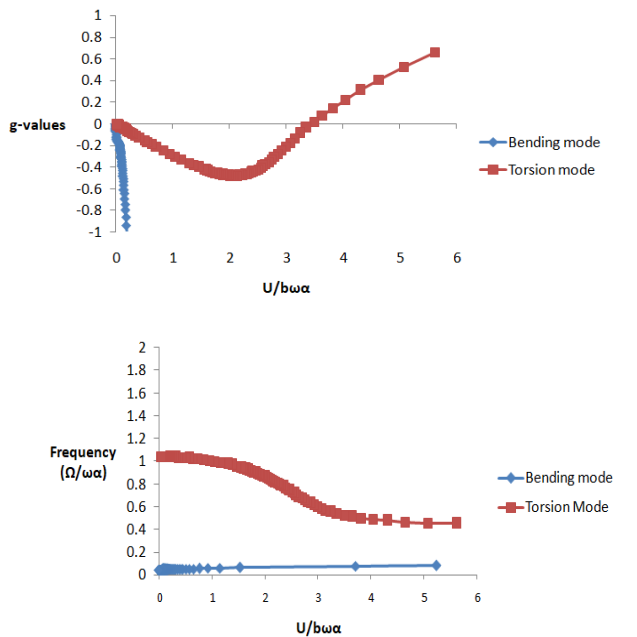


Figure 13 U-g and U-frequency diagram for the aft wing.

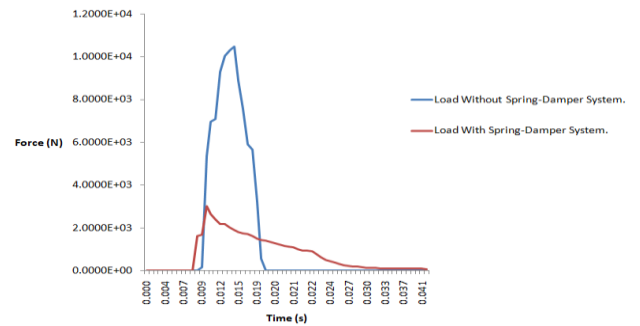
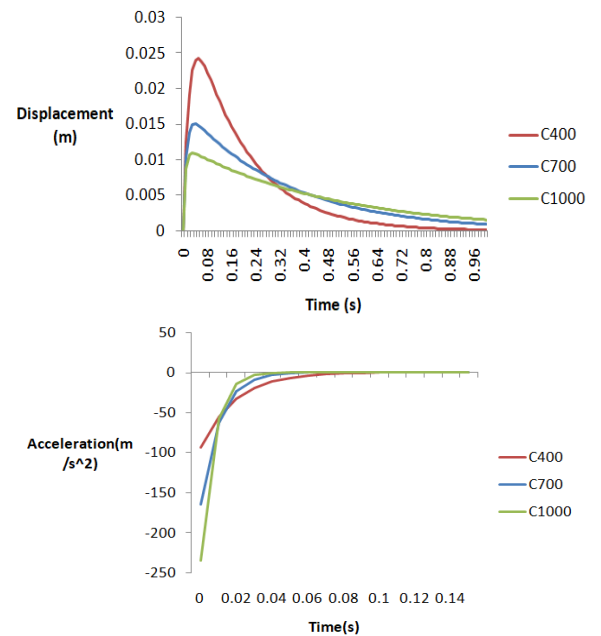


Figure 14 Impact forces experienced by the landing gear system.

Among the major parts of an aircraft, the wings are the ones that are highly stressed and where flutter mostly occurs also. But since flutter is a complicated phenomenon, it should be treated in a separate analysis. In this study, the flutter analysis used was the V-g analysis where it is assumed to have one unknown value,  $g$ . In Figures 12 and 13, the results for two modes (bending and torsion) of front and aft wings are shown, respectively, in the form of frequency versus velocity and damping versus velocity curves. In Figures 12 and 13, the velocity that passes through  $g = 0$ , is the flutter velocity of the model. The flutter frequency of the



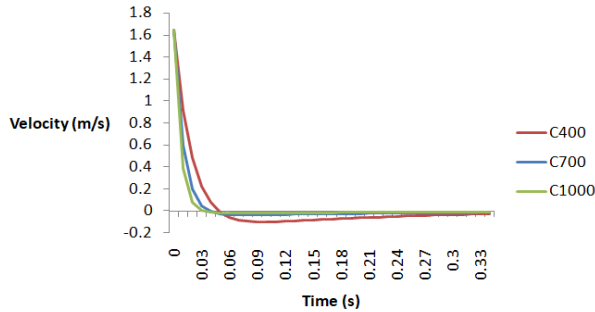


Figure 15 Spring-damper model response in displacement, velocity and acceleration.

model can then be determined using the right-side plots of Figures 12 and 13 and picking off the frequency value of the unstable mode at the flutter velocity value. The slope of the damping versus velocity curve represents the behavior of the oscillation. The flutter non-dimensional speed of the front wing based on the result is 3.94, this corresponds to 37.23 m/s. For the aft wing, the flutter non-dimensional speed is 3.36, which then corresponds to 30.164 m/s. With the calculated dive speed of 25 m/s, and the addition of wing-tip in the design, we can say that there is still a safe margin for the flutter speed. Below the calculated speed, it is expected that any excitation that may lead to vibration will be damped. Beyond that speed, violent vibrations will occur and the coalescence of modes of vibration will damage the wing.

A fatigue analysis was also conducted on the wings and it was found out that the designed box-wing configuration could reach up to  $2.438 \times 10^6$  cycles before any noticeable damage in the wing structures.

Lastly, safe and successful landing is the completion phase of any flight mission. The impact forces on the aircraft during landing simulations were too large that they could potentially damage the payload instruments and the whole aircraft structure. Because of these results, a spring-damper system was incorporated to the landing gear of the UAV which effectively reduced the impact load from the original 10,487 N down to only 3,016.8 N, that is 71.23% as can be seen in Figure 14. From the three spring-damper systems being considered, C400 provides the smoothest landing because of its long stroke and non-abrupt deceleration as can be readily seen in Figure 15.

#### 4 CONCLUSIONS

Within the limit load factor  $n$  equal to 1.4, the designed canard box-wing UAV could withstand the aerodynamic loadings during flights typical for disaster management and agricultural surveillance applications. Even with the introduction of a sharp-edged gust of

5 m/sto simulate flight condition disturbance, the designed UAV could still perform its assigned mission safely. It was observed that the deflections on the aft and front wings both in static and dynamic loadings were very minimal. The addition of a spring-damper system significantly improved its landing performance. The overall computational structural analysis conducted on the novel UAV with canard and Prandtl box-wing configuration has shown significant results satisfying the set design requirements and has verified the frozen conceptual design made in the previous study [8]. The next phase of the UAV development, which is on the experimental validation of the integrity of the UAV airframe structure and components, can now proceed with confidence because of the remarkable results obtained in this computational structural study. The integration of UAVs in various civilian applications is rapidly growing and is gaining popularity due to its immense contribution in the optimization of data acquisitions thereby increasing the productivity of its operations. Today, drones are very in demand in agricultural applications. However, a fixed-wing aircraft such as the model used in this study can fly longer, at a higher altitude, can carry larger payload thus making this more ideal to conduct mapping and crop spraying to name a few.

#### ACKNOWLEDGEMENT

This study was supported by Engineering Research and Development for Technology (ERDT) Program of the Department of Science and Technology (DOST) at the College of Engineering of Mindanao State University-Iligan Institute of Technology (MSU-IIT) in Iligan City.

#### REFERENCE

- [1] Austin, R. (2010). "Unmanned Aircraft Systems: UAVs Design, Development and Deployment". West Sussex, UK: John Wiley & Sons Ltd.
- [2] Barnhart, R. K., et al., (2012). "Introduction to Unmanned Aircraft Systems".
- [3] Blom, J. D. (2010). "Unmanned Aerial Systems: A Historical Perspective". Leavenworth, Kansas: Combat Studies Institute Press.
- [4] Chiu, W. K., et al., (2016) "Large structures monitoring using unmanned aerial vehicles" *Procedia Engineering* 188 (2017) 415 – 423.
- [5] Donaldson, B. (2008). "Analysis of Aircraft Structures An Introduction".

- [6] Esfahlani, S. S. (2018). "Mixed reality and remote sensing application of unmanned aerial vehicle in fire and smoke detection". *Journal of Industrial Information Integration* 15 (2019) 42-49.
- [7] Estrada, R. M. and Ndoma, A. (2019). "The uses of unmanned aerial vehicles –UAV's- (or drones) in social logistic: Natural disasters response and humanitarian relief aid" *Procedia Computer Science* 149 (2019) 375–383.
- [8] Estrada, M. A. R. (2011). "Policy modeling: Definition, classification and evaluation" *Journal of Policy Modeling* 33 (2011) 523–536.
- [9] Jemitola, P. O. (2012). "Conceptual Design and Optimization Methodology for Box Wing Aircraft". *PhD Thesis*. Cranfield, UK: School of Aerospace Engineering, Cranfield University.
- [10] Khan, F. A. (2010). "Preliminary Aerodynamic Investigation of Box-Wing Configurations Using Low Fidelity Codes". *MS Thesis*. Luleå, Sweden: Luleå University of Technology.
- [11] Kundu, A. K. (2010). "Aircraft Design". New York: Cambridge University Press.
- [12] Liu, D., Piolenc, F., Sarhaddi, D. (1997). "Flutter Prevention Handbook: A Preliminary Collection".
- [13] Megson, T.H. G. (2010) "An Introduction to Aircraft Structural Analysis".
- [14] Meier, P. (2015). "Digital Humanitarians". Available here: <https://bit.ly/2reHsUg>
- [15] Mogili, U.M. and Deepak, BBVL (2018) "Review on Application of Drone Systems in Precision Agriculture". *Procedia Computer Science* 133 (2018) 502–509.
- [16] Padua, L., et al. (2017). "Very high-resolution aerial data to support multi-temporal precision agriculture information management" *Procedia Computer Science* 121 (2017) 407–414.
- [17] Phillips, W., et al. (2000). "Modern Adaptation of Prandtl's Classic Lifting-Line Theory" *JOURNAL OF AIRCRAFT* Vol. 37, No. 4, July–August 2000.
- [18] Raymer, D. P. (1992). "Aircraft Design: A Conceptual Approach". USA: AIAA.
- [19] Remocaldo, G.(2015). "Conceptual Design And Aerodynamic Performance Analysis Of A Canard Box-Wing Unmanned Aerial Vehicle (UAV) Platform for Aerial Photography And Surveillance Applications". *MS Thesis*. Mindanao State University – Iligan Institute of Technology.
- [20] Roskam, J. (2004). "Airplane Design Part I: Preliminary Sizing. Kansas USA: Design, Analysis and Research Corporation".
- [21] Shumao, W., et al. (2018). "Research on the prediction model and its influencing factors of droplet deposition area in the wind tunnel environment based on UAV spraying ". *IFAC PapersOnLine* 51-17 (2018) 274–279.
- [22] Srinath, R., et al. (2017). "Aerodynamic Analysis of Forward Swept Wing Using Prandtl-D Wing Concept" *International Journal of Engineering Trends and Technology (IJETT) – Volume 54 Number 2* (2017).
- [23] Sudhakar, S., et al. (2019). "Unmanned Aerial Vehicle (UAV) based Forest Fire Detection and monitoring for reducing false alarms in forest-fires" *Computer Communications* 149 (2020) 1–16.
- [24] Tatum, M. C. and Liu, J. (2017) "Unmanned Aircraft System Applications In Construction" *Procedia Engineering* 196 (2017) 167 – 175.
- [25] Wang, X. et al. (2018). "Development of Visualization System for Agricultural UAV Crop Growth Information Collection" *IFAC PapersOnLine* 51-17 (2018) 631–636.
- [26] Wang, X. et al. (2018). "Simulation Analysis of Airfoil Deformation of Agricultural UAV under Airflow Disturbance Based on ANSYS" *IFAC PapersOnLine* 51-17 (2018) 826–830.
- [27] Wood Handbook, Wood as an Engineering Material (2010).
- [28] Zafirov, D., (2014). "Closed Wing Aircraft Classification" *International Journal of Engineering Research & Technology (IJERT)* Vol. 3 Issue 1, January – 2014.
- [29] Zhao, T., et al., (2016). "More Reliable Crop Water Stress Quantification Using Small Unmanned Aerial Systems (sUAS)" *IFAC-PapersOnLine* 49-16 (2016) 409–414.